THE BELL SYSTEM TECHNICAL JOURNAL
Vol. 62, No. 10, December 1983
Printed in U.S.A.

The AR6A Single-Sideband Microwave Radio System:

Predistortion for the Traveling-Wave-Tube Amplifier

By R. P. HECKEN,* R. C. HEIDT,* and D. E. SANFORD*

(Manuscript received February 7, 1983)

To satisfy the single-sideband amplitude-modulated system noise requirements, the transmitter must be very linear. Predistortion reduces intermodulation distortion of the transmitter to acceptable levels. This paper deals with the design considerations, the model of the transmitter used to analyze third-order intermodulation products, and the methods applied to align the predistorter-transmitter combination for effective intermodulation reduction.

I. INTRODUCTION

The frequency stability required for single-sideband amplitude-modulated (SSB-AM)† system operation results in the potential for in-phase addition of intermodulation noise from repeater to repeater. Traveling-Wave Tubes (TWTs) offer the best linearity (and, consequently, the lowest intermodulation distortion) available for currently existing 6-GHz power amplifiers. However, linearity must be improved to satisfy system noise requirements.

The concept of predistortion to reduce intermodulation distortion

*Bell Laboratories.

†Acronyms and abbreviations used in the text and figures of this paper are defined at the back of this *Journal*.

had originally been explored extensively at 4 GHz[1] and was found considerably less complex than feedforward.[2] In particular, predistortion at intermediate frequencies appeared attractive because of its simplicity and economy. Operating at intermediate frequency (IF), the predistorter is placed ahead of the up converter and is, therefore, able to cancel intermodulation products generated in the converter and the traveling-wave tube. Clearly, the latter is the major contributor to nonlinear distortions and will be treated accordingly.

Extensive measurements have shown that TWTs, if operated at low radio frequency (RF) power levels, i.e., in a domain of weak nonlinearity, behave essentially as first- and third-order devices and produce odd-order intermodulation products within the narrow frequency band of interest. In the AR6A* System the predistorter is designed to cancel distortions in this power region, and it is important to distinguish this mode of operation from other methods where predistortion is analyzed in a region of strong nonlinearity.[3,4]

In the following section we will proceed with a simple analysis of nonlinearities of the transmitter, which is based on a model that proved to be very accurate within the useful power range of the AR6A System. Section III will deal with practical design considerations, and in Section IV we will conclude with the results.

II. NARROWBAND DISTORTION ANALYSIS

2.1 Nonlinear model of the traveling-wave tube

Measurements on a large number of traveling-wave tubes having a saturated power-handling capability from 5 to 20W showed that even at very low RF power levels (<1W), the simple memory-free polynomial model describing gain nonlinearity of the TWT is inadequate. Two additional effects must be included in the analysis to achieve substantial intermodulation reduction of 20 dB or more: the amplitude and phase distortions due to reactive circuit elements and the amplitude modulated to phase modulated (AM-PM) conversion effect. A model of the TWT that was found very useful is shown in Fig. 1. This model characterizes a special class of nonlinear systems in which a memory-free, nonlinear two-port network is embedded between two linear passive two-port networks having the impulse responses $h_A(t)$ and $h_B(t)$, respectively. For narrowband systems the nonlinear two-port is well modeled by a finite odd-order power series in two variables with constant coefficients[5,6]

$$w = b_1' u + b_3' u^3 + b_5' u^5 + \cdots + b_1'' \dot{u} + b_3'' \dot{u}^3 + b_5'' \dot{u}^5 + \cdots, \quad (1)$$

*Amplitude Modulation Radio at 6 GHz for the initial (A) version.

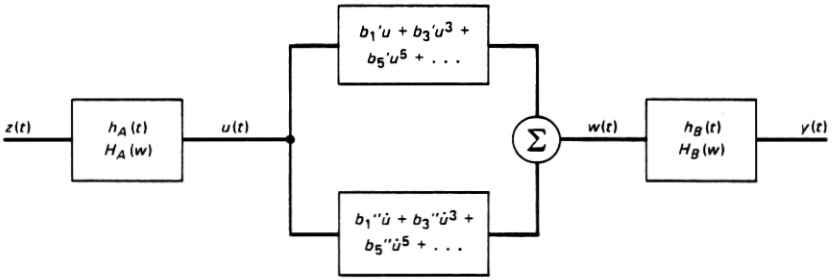

Fig. 1—Approximate model of a traveling-wave-tube amplifier with weak nonlinearities.

where $\dot{u} = du/dt$. The partial series in powers of $\dot{u}$ accounts for AM-PM conversion. An important aspect of this TWT model is the fact that the two interfaces between the three two-ports are, in general, not accessible.

For our analysis, we will limit the power series to first- and third-order terms. Applying the Fourier transformation to eq. (1), we obtain the complex nonlinear input-output relation

$$W = B_1 U + B_3 U^{3*} + \cdots, \tag{2}$$

with the notation U^{3*} indicating the repeated convolution $U*U*U$. The complex coefficients are given by

$$B_1 = b_1' + j\omega_c b_1'', \tag{3a}$$

and

$$B_3 = b_3' - j\omega_c^3 b_3''. \tag{3b}$$

The narrowband assumption manifests itself in eq. (3), in that the frequency variable, ω, has been replaced by the constant channel frequency, ω_c, while performing the convolutions. With the input-output relations for the nonlinear portion of the TWT established, we can write the overall transfer function for the TWT model. Let Z and Y be the Fourier transforms of the input and output signals; then

$$Y = H_B B_1 H_Z Z + H_B B_3 (H_A Z)^{3*} + \cdots, \tag{4}$$

where H_A and H_B are the transfer functions of the input and output networks, respectively. Before we proceed with the distortion analysis of the transmitter, we need first to discuss some properties of the up converter.

2.2 The Schottky modulator

Comparative measurements on Varactor Diode Converters (VDC) and Schottky Diode Converters (SDC) have shown the superiority of

the latter when considering its nonlinear distortion characteristics versus RF output power. These measurements revealed that the SDC, when pumped with high local oscillator power, behaves like a third-order device over a wide range of RF signal levels. This property is indeed useful because it allows the predistorter, tailored to compensate for third-order distortions, to improve the converter distortions as well. Moreover, because of its conversion loss, in contrast to the conversion gain of a VDC, a higher level of distortions can be tolerated in an SDC. This is so because, for a given performance, the TWT essentially limits the RF output power. To illustrate this, we compute the power of a three-tone, third-order product generated in the converter as it appears at the output of the TWT. If we refer to Fig. 2 this power is

$$P_{A+B-C} = M_{A+B-C} + 3P_A + G \qquad \text{(dBm)}, \tag{5}$$

where M_{A+B-C} is the particular intermodulation coefficient[7] in decibels of the converter, P_A is the power in dBm of each of the equal-level, three-tones at the output of the converter, and G is the overall gain of the bandpass filter (BPF) and TWT. Since the single-tone power at the tube output is

$$P_{AO} = P_A + G \qquad \text{(dBm)}, \tag{6}$$

we find that

$$P_{A+B-C} = M_{A+B-C} - 2G + 3P_{AO} \qquad \text{(dBm)}. \tag{7}$$

Thus, for a specified performance (P_{AO} fixed) the device distortion M_{A+B-C} can be reduced by 2 dB for each decibel increase in TWT gain. Since the difference in conversion loss and gain can be as high as 12 dB, the Schottky diode converter may have an M_{A+B-C} that could be 24 dB worse than that of a varactor diode converter, yet may still yield the same distortion performance. Typically, the SDC has an M_{A+B-C} of about −25 dB compared to −40 dB of the VDC, which clearly shows the disadvantage of the varactor diode converter.

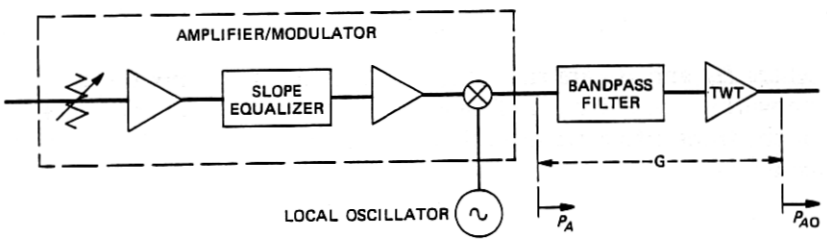

Fig. 2—Simplified block diagram of the AR6A amplifier/modulator with bandpass filter and traveling-wave tube.

It is useful to compare the distortion power generated by the converter to that of the TWT. At a total signal output power of +27 dBm for three equal-level tones, the single-tone power P_{AO} is approximately +22 dBm. With $G = 45$ dB and $M_{A+B-C} = -25$ dB from eq. (7), $P_{A+B-C} = -49$ dBm. A TWT having an $M_{A+B-C} = -91$ dB generates intermodulation power of the same product at a level of −25 dBm. Obviously, one can ordinarily neglect the contribution of the converter since it increases the total intermodulation power by only 0.53 dB. However, if the predistorter can reduce distortions by more than 20 dB, the converter will contribute significantly to the resulting intermodulation noise unless the predistorter also reduces its nonlinearities. In spite of this, to keep our discussion simple we will not include the converter-generated distortions in our analysis.

2.3 Generalized nonlinear transmitter model

The mathematical treatment of the nonlinearities of the complete transmitter is complicated, even when we neglect the converter nonlinearities, because of the operation in two frequency domains. As is shown in the appendix, the frequency translation from IF to RF requires each sideband to be considered separately. We will point out the differences where appropriate and develop the analysis for the upper sideband only. To arrive at a tractable model of the complete transmitter, we actually include the converter, bandpass filter, etc., in the TWT model as described in the appendix. Frequency characteristics at RF are then referred to the IF band, allowing the predistorter to be directly connected to this TWT model. The cascade of predistorter with IF amplifiers and the converter with bandpass filter, TWT, etc., is depicted in Fig. 3, where we used a nonlinear model of the predistorter that is similar to that of the TWT. Thus, we assume that the predistorter has the transfer function

$$Z = G_B A_1 G_A X + G_B A_3 (G_A X)^{3^*}, \tag{8}$$

which leads to the following overall transfer function for the upper sideband (USB):

$$Y_{\text{USB}} = H_B B_1 H_A G_B A_1 G_A X + H_B B_1 H_A G_B A_3 (G_A X)^{3^*} + H_B B_3 (H_A G_B A_1 G_A X)^{3^*} + \cdots. \tag{9}$$

In eq. (9) all terms requiring higher than third-order convolutions have been neglected. Two observations can be made immediately: the distortion terms depend directly or indirectly on the product $G_A X$ as part of the convolution process. Thus, the frequency characteristic of the input network of the predistorter will have no effect on the minimization of these terms. Also, H_B is a factor in both distortion

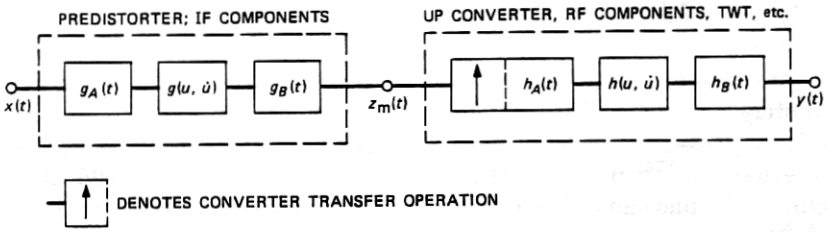

Fig. 3—A generalized model of the AR6A transmitter.

terms, indicating that the frequency characteristic of the TWT output network also has no effect on the intermodulation cancellation. For the purpose of this analysis we can, therefore, set $G_A = 1$ and $H_B = 1$. With these simplifications the third-order distortion term becomes, in the case of the upper sideband,

$$D_3 = B_1 H_A G_B A_3 (X)^{3^*} + B_3 (H_A G_B A_1 X)^{3^*} \qquad \text{(USB)}. \tag{10}$$

It can be shown that in order for D_3 to at least vanish over the frequency band where X exists, it is necessary for the product $H_A G_B A_1$ to have constant magnitude and constant delay as function of frequency within that band, i.e., the condition must be met

$$H_A G_B A_1 = C e^{-j\omega\tau}, \tag{11}$$

where

$$C = |H_A G_B A_1| \qquad \text{and} \qquad \omega\tau = \measuredangle(H_A G_B A_1).$$

This yields for D_3

$$D_3 = \left(B_1 \cdot \frac{A_3}{A_1} C e^{-j\omega\tau} + B_3 C^3 e^{-j\omega\tau} \right) X^{3^*}.$$

Hence, frequency-independent cancellation of the third-order distortions at the upper sideband is possible if, in addition to eq. (11), the following condition is fulfilled:

$$\frac{A_3}{A_1} = -\frac{B_3}{B_1} \cdot |H_A G_B A_1|^2 \qquad \text{(USB)}. \tag{12a}$$

The corresponding condition for the lower sideband (LSB) is

$$\frac{A_3}{A_1} = -\frac{\check{B}_3}{\check{B}_1} \cdot |H_A G_B A_1|^2 \qquad \text{(LSB)}, \tag{12b}$$

where $\check{B}$ is the complex conjugate of B. Thus, the required complex ratios A_3/A_1 for the LSB and USB are conjugate to each other. The

fundamental relationships for wideband distortion cancellation are described in eqs. (11) and (12). Therefore, design as well as alignment procedures are essentially based on these criteria. Obviously, eq. (11) requires amplitude and delay equalization for all components in the signal path between the nonlinear element of the predistorter and the nonlinear region of the TWT, unless these components have inherently flat response and constant delay. In the AR6A transmitter, however, a certain amount of slope equalization was required to achieve intermodulation improvement by more than 30 dB. This equalizer is integrated into the modulator/amplifier unit.

From eqs. (12a) and (12b) we derive the required magnitude and phase of the distortions to be generated in the predistorter. The magnitude is practically independent of the sideband used since the TWT generates approximately the same intermodulation level at both frequencies. Therefore,

$$|A_3| = \left| \frac{B_3}{B_1} \right| \cdot |A_1|^3 \cdot |H_A G_B|^2. \tag{13}$$

It is obvious that for stable operation of the predistorted transmitter, the magnitude of the transfer coefficients, $|A_1|$ of the predistorter and $|H_A G_B|$ of the interconnecting networks (which includes the up converter), must be very well controlled and remain stable over time and temperature. The same is true for the gain of the TWT, represented by $|B_1|$ in eq. (13).

The phase condition for the upper sideband is

$$(\sphericalangle A_3 - \sphericalangle A_1) = \pi + (\sphericalangle B_3 - \sphericalangle B_1) \qquad \text{(USB)}, \tag{14a}$$

and for the lower sideband is

$$(\sphericalangle A_3 - \sphericalangle A_1) = \pi - (\sphericalangle B_3 - \sphericalangle B_1) \qquad \text{(LSB)}. \tag{14b}$$

Thus, means have to be provided in the predistorter to achieve both phases since either the USB or LSB may be deployed, depending on the channel, in the AR6A System.

2.4 Interaction distortions

In the derivation of the overall nonlinear transfer function for the transmitter, terms involving convolutions of higher than third order have been neglected. It is worthwhile, however, to discuss the next higher-order term, which is found to be

$$D_5 = 3B_3(H_A G_B A_1 X)^{2^*} * (H_A G_B A_3)(X)^{3^*}. \tag{15}$$

Assuming that the transmitter is aligned properly, such that conditions in eqs. (11) and (12) are fulfilled, the magnitude of D_5 becomes

$$|D_5| = 3|H_A G_B A_1|^5 \cdot \left| \frac{B_3^2}{B_1} \right| \cdot |X^{5^*}|. \tag{16}$$

We see from the above expressions that this fifth-order distortion is strictly due to interaction between the third-order terms of the predistorter and TWT and that the magnitude is very sensitive to the first- and third-order coefficients of the TWT. For $|D_5|$ to remain small, $|B_1|$ (i.e., TWT gain) should be large and $|B_3|$ of the device must be small at the outset.

2.5 *Residual third-order distortions*

In practice it is not possible to fulfill the conditions given by eqs. (11) and (12) at all frequencies. It becomes necessary, therefore, to estimate the amount of residual distortions after imperfect predistortion. In particular, the effect of deviations from the ideal condition in eq. (11) is important because of the strong sensitivity of D_3, defined in eq. (10), to the transfer function $T = H_A G_B A_1$. We will, therefore, attempt to analyze $|D_3|$ as a function of small deviations δ_c and δ_α of $|T|$ and $\alpha = \measuredangle T$, respectively. Thus, we express T as

$$T = (C + \delta_c) \cdot e^{-j(\omega\tau + \delta_\alpha)}, \tag{17a}$$

which is approximately equal to

$$T \simeq Ce^{-j\omega\tau} + (\delta_c/C - j\delta_\alpha)Ce^{-j\omega\tau}$$

or

$$T \simeq T_o + E \cdot T_o. \tag{17b}$$

Obviously, $T_o = C \cdot e^{-j\omega\tau}$ represents the ideal transfer function, which we will assume to fulfill the condition in eq. (11). The error term $E \cdot T_o$ is proportional to the complex quantity

$$E = \frac{\delta_c}{C} - j\delta_\alpha, \tag{18}$$

and is a function of frequency. Introducing eq. (17b) into eq. (10) we obtain

$$D_3 = B_1 \frac{A_3}{A_1} (T_o + ET_o)(X)^{3^*} + B_3(T_o X + ET_o X)^{3^*}. \tag{19}$$

Performing the convolutions on the last term, eq. (19) can be expressed as

$$D_3 = B_1 \frac{A_3}{A_1} T_o(X)^{3^*} + B_3 C^2 T_o(X)^{3^*} + D_{3R}. \tag{20}$$

With the predistorter active and conditions in eqs. (11) and (12)

being met, the first two terms cancel. The residual distortions are then approximately given by

$$D_{3R} = B_1 \frac{A_3}{A_1} ET_oX^{3^*} + 3B_3(T_oX)^{2^*} * (ET_oX) + \cdots, \qquad (21)$$

where terms of higher order in (ET_oX) have been neglected. By introducing eq. (12) and using the identity $(T_oX)^{2^*} = CT_o(X)^{2^*}$ we obtain

$$D_{3R} = -B_3C^2T_o[EX^{3^*} - 3X^{2^*} * (Ee^{-j\omega\tau}X)]. \qquad (22)$$

The power spectrum of D_{3R} for given deviations E can be computed using eq. (22). Unfortunately, this involves, in general, complex numerical calculations and results do not easily provide further insight. Instead, we have used eq. (22) to arrive at an upper bound for the magnitude of D_{3R}. By using the inequality

$$|D_{3R}| \leq |B_3| \cdot C^3[|E| \cdot |X^{3^*}| + 3|X^{2^*}| * |E \cdot X|] \qquad (23)$$

we have examined each term within the brackets individually for two typical, yet simplified, error functions E.

2.5.1 Case 1—Out-of-band residual distortions

If we assume that $|E|$ and $|X|$ are as illustrated in Fig. 4, it becomes obvious that only the first term in eq. (23) contributes to residual distortions, because the product $E \cdot X$ vanishes everywhere. Typically, the bandpass filter between converter and TWT produces this type of residual out-of-band third-order distortion. In the AR6A System, their

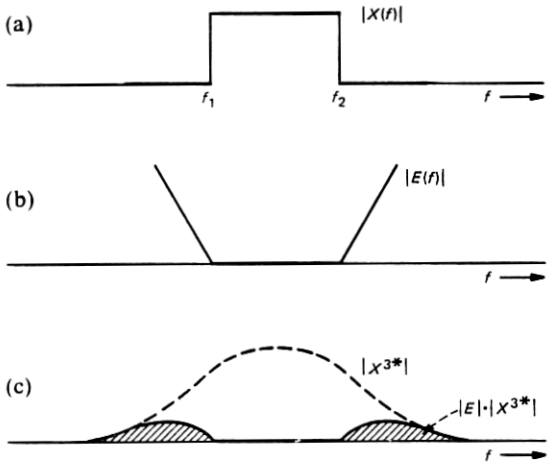

Fig. 4—Out-of-band distortions with perfect in-band predistortion: (a) input spectrum; (b) deviation from flatness; (c) distortion spectrum.

level is sufficiently small to cause no interference with other radio channels.

2.5.2 Case 2—In-band residual third-order distortions

This important case deals with parabolic in-band deviations E, as illustrated in Fig. 5. Satisfactory, but imperfect, tuning of the RF bandpass filter or insufficient flatness of the IF driver amplifier in the converter are primary causes for parabolic-type residual deviations. For simplicity, we approximate these by a triangular distribution, which causes the in-band residual distortions as shown shaded in Figs. 5c and 5d. It is important to recognize that the level of distortions due to the second term of eq. (23) varies in direct proportion to the fractional bandwidth Δf over which $|E|$ assumes a substantial magnitude. This is in contrast to the contribution stemming from the first term, the maximum level of which is only proportional to the magnitude of E. As a rule of thumb, the first term dominates if

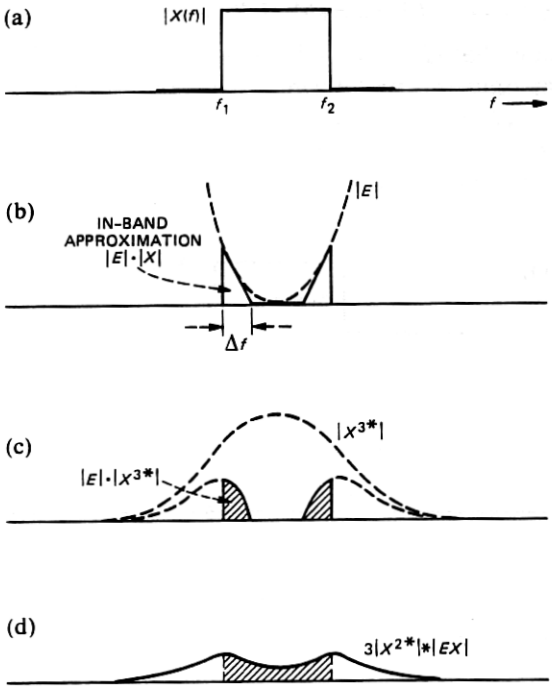

Fig. 5—Residual in-band third-order distortion spectrum: (a) input spectrum; (b) deviation from flatness; (c) residual distortion spectrum, first term, eq. (23); (d) residual distortion spectrum, second term, eq. (23).

$$3\Delta f < \tfrac{1}{4} \cdot BW,$$

where BW is the bandwidth of the input spectrum, i.e., $BW = f_2 - f_1$. In the AR6A System a special slope equalizer has been incorporated into the driver amplifier of the up converter to ensure that essentially only parabolic residual deviations remain at the very edges of the signal band, thus, keeping Δf as small as practicable.

The maximum tolerable amount of these deviations has been derived from eq. (23) by requiring that the ratio $|D_{3R}/D_{3o}|$ is below a specified level, where $|D_{3o}| = |B_3|C^3|X^{3^*}|$ represents the unpredistorted intermodulation spectrum within the message band. Thus, this ratio is a direct measure of distortion reduction. The predistortion improvement (PDI) in decibels is given by

$$PDI = -20 \log|D_{3R}/D_{3o}| \qquad \text{(dB)}. \tag{24}$$

If only the first term in eq. (23) contributes to residual distortions, the predistortion improvement becomes

$$PDI = -10 \log\left[\left(\frac{\delta_c}{C}\right)^2 + \delta_x^2\right] \qquad \text{(dB)}.$$

Figure 6 shows plots of constant PDI values as a function of phase deviation (in degrees) and flatness, defined as $20 \log(1 \pm \delta_c/C)$. We see that to achieve a PDI $\geq$ 40 dB, the flatness must be better than ± 0.06 dB and phase linearity is required to be within ± 0.4 degree, provided both deviations contribute equal amounts.

Deviations in other coefficients describing the transmitter model, in particular A_1, A_3 and B_1, B_3, have been treated similarly. Except for A_1, their effect is less complicated because they are not convolved. It can be shown that as long as the residual distortions are caused only by nonconvoluted terms, the total amount of residual distortions is bound by the inequality

$$\left|\frac{D_{3R}}{D_{3o}}\right| \leq \sqrt{\left(\sum_{i=1}^{N} |m_i|\right)^2 + \left(\sum_{i=1}^{N} |\Delta\psi_i|\right)^2}, \tag{25}$$

where m_i represents the deviation from flat magnitude and $\Delta\psi_i$ the deviation from phase linearity of the ith contributing coefficient. This upper bound estimate given by eq. (25) is very conservative because it is based on the assumption that at any frequency all deviations of the different component parts are causing in-phase addition. This is, in general, not true and a more useful estimate based on statistical addition is

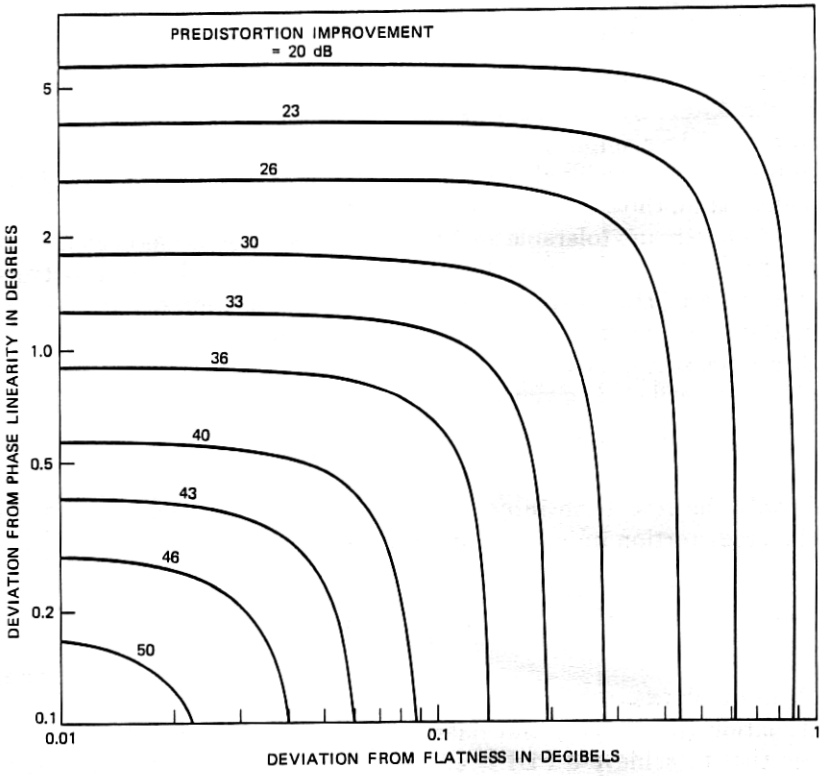

Fig. 6—Contours of constant predistortion improvement.

$$\left| \frac{D_{3R}}{D_{3o}} \right| \equiv \sqrt{\sum_{i=1}^{N} |m_i|^2 + \sum_{i=1}^{N} |\Delta\psi_i|^2}. \tag{26}$$

For the AR6A transmitter, under nominal testing conditions, the objective was to achieve a PDI of at least 30 dB over the full 30-MHz band. Allowing an additional margin of 3 dB and allocating equal deviations to each of the five possible contributors in the transmitter model (namely, A_1, A_3, B_1, B_3, and the product $H_A G_B$) results in a flatness requirement within ±0.06 dB and phase linearity requirement within ±0.4 degree. (Using the conservative upper bound would yield ±0.03 dB and ±0.18 degree as requirements on the model coefficients.) Since the coefficients A_1 and A_3 are only representative of the various components in the predistorter, its actual circuit requirements have been set at nominally ±0.02 dB for flatness. The corresponding requirements for phase linearity are then automatically met because of the minimum phase property of the circuits used.

III. PRACTICAL DESIGN CONSIDERATIONS

3.1 Components

The predistorter comprises components operating over the 30-MHz bandwidth centered at 74.1 MHz. The predistorter is described in the block diagram shown in Fig. 7. The key component is the nonlinear generator referred to as the cuber.[8] It consists of four back diodes arranged in a bridge configuration so that signals incident at the input of the network are attenuated by approximately 60 dB at the output. The amplitude of each third-order complementary distortion term at the cuber output is related to the amplitudes of the input signals at frequencies A, B, and C by

$$P_{A+B-C} = 46.6 + P_A + P_B + P_C \qquad \text{(dBm)}. \tag{27}$$

The driver amplifier at the input to the predistorter provides gain so that the input signal to the cuber is at the optimum level. The optimum is dictated by choosing the drive such that the cuber does not generate fifth-order distortion terms that would exceed the level assumed in eq. (9). The distortion amplifier provides gain so that the complementary distortion terms generated by the cuber have the required amplitude. The gain in the distortion amplifier must be limited because of the addition of thermal noise back into the main path. The distortion adjustment potentiometer in the output coupler is used to fine tune the amplitude to provide the exact value of $|A_3|$ required for each individual transmitter.

The phase of the third-order complementary distortion terms generated in the cuber is established by the phase resolver network.[9] This network is designed to provide a constant-phase linear-phase difference between the two output ports and has the adjustment capability to cover the range of phase angles required. The output ports of the

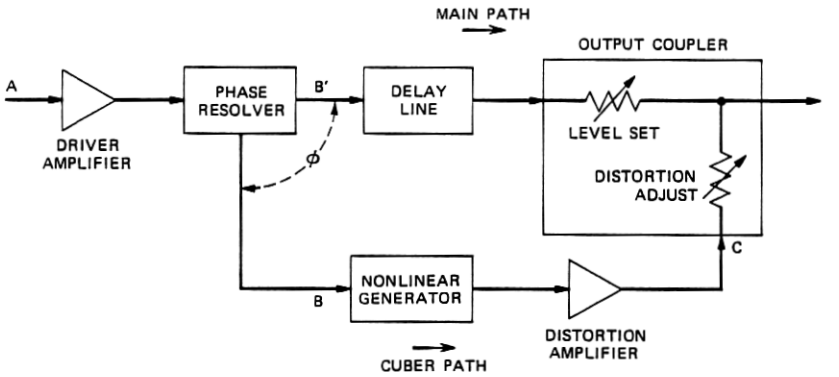

Fig. 7—Predistorter block diagram.

resolver network are arranged so that the connections to these ports can be interchanged. By doing so, the predistorter is adaptable for either USB or LSB operation.

The delay line in the main path is added to match the delay of the cuber path. To account for tolerances of the components, a delay adjustment is required during the manufacturing procedure so that the delays of the two paths are matched as closely as possible.

Because of the large amount of delay required, mismatches at the ends of the delay line result in shape over the 30-MHz channel that is difficult to equalize. Thus, the return loss of the appropriate ports of the delay line, phase resolver, and output coupler is carefully controlled.

3.2 Equalization

Transmission deviations from a flat shape in either the main or cuber path result in residual third-order distortion. Two slope equalizers in the predistorter are employed to control the linear portion of the deviations.

The first slope equalizer adjusts the path from point A to point B, as shown in Fig. 7. This slope equalizer is part of the driver amplifier. The end points over the 30-MHz channel are equalized within ±0.02 dB. This procedure imposes strict shape requirements on the resolver network so that

$$|H_{AB}| \cong |H_{AB}'|. \tag{28}$$

The second slope equalizer adjusts the path from point B to point C. This slope equalizer is part of the distortion amplifier. The equalization process is accomplished by first disabling the bridge network in the cuber, then equalizing the end points over the 30-MHz channel to within ±0.02 dB.

3.3 Alignment of transmitter

Since each predistorter is equalized during the manufacturing process as previously discussed, the rest of the transmitter must be equalized after all the parts are assembled. From eq. (11) these separate equalizations are equivalent to requiring that H_A be aligned in the transmitter configuration while $G_B A_1$ is aligned separately.

From Figs. 2 and 3, we see that H_A includes the amplifier/modulator, bandpass filter, and the input network of the TWT. A slope equalizer is incorporated in the amplifier/modulator. It is clear that the interface of this portion of the transmitter is somewhere within the active portion of the TWT and is, therefore, not accessible using standard methods. A special scanning intermodulation (IM) test set[10] was designed to permit this measurement to be made. The scanning

capability of the test set permits the transmission path to be slope equalized over the 30-MHz channel.

The overall result of the equalization process is measurable using the scanning IM test set to measure the predistortion improvement across the band. The results of a number of such measurements are summarized in Fig. 8. Two types of TWTs have been used in the AR6A transmitter. For the transmitters using the WE 473A TWT, the average PDI for 24 TWTs indicates a minimum value of 33 dB. To obtain this result, the deviation from flatness must be approximately 0.1 dB. For the transmitters using the KS-22469 TWT, the average PDI for 27 TWTs indicates a minimum value of 35 dB with the corresponding deviation from flatness being approximately 0.07 dB.

Final measurements are made using the scanning IM test set on each transmitter. At this time approximately 3000 units have been produced. The results still show an average minimum PDI of approximately 35 dB.

IV. PERFORMANCE

4.1 Variation with time

Predistortion of the traveling-wave tube has been demonstrated in the laboratory and manufacturing environment. Transmitter perform-

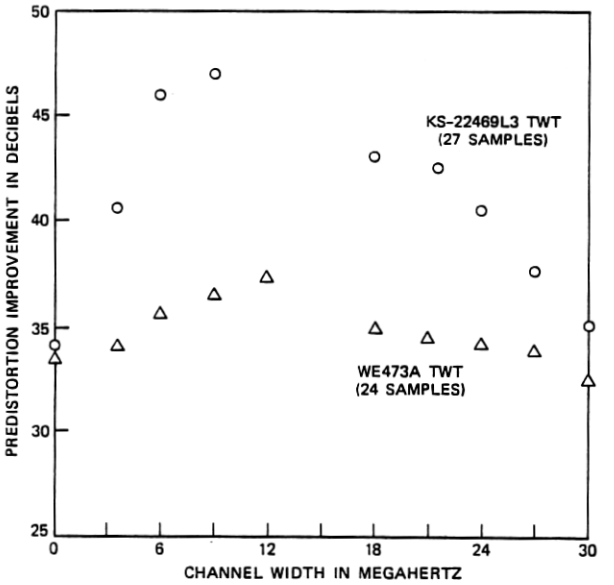

Fig. 8—Average predistortion improvement across a channel.

ance in the field with time and temperature is being tracked by observing the AR6A System in its operating environment.

Data accumulated over a period of several years for 25 TWT amplifiers indicate that the performance with time largely depends upon the stability of the TWT and power supply. The change of gain of the TWT amplifier has been, in general, less than 0.35 dB per year (corresponding to a PDI of 22 dB). Exceptions exist; some amplifiers have demonstrated very large (>2 dB) gain changes. Although no regular monitoring plan has been established, occasional evaluation of selected channels has corroborated the stability estimates.

4.2 Variation with temperature

Temperature changes also cause transmitter gain variation and, therefore, cause the PDI to vary. The AR6A transmitter was tested over an ambient temperature range from 40 to 120°F. These tests revealed that the variation of the PDI was due to transmitter gain changes. The largest contributor to the gain change is the TWT amplifier. Separate tests of five amplifiers established an average change of 0.35 dB over the temperature range. For a transmitter aligned at 80°F, this type of gain variation results in a worst-case PDI of 27 dB.

4.3 Summary

In some cases, gain variations with time and temperature significantly exceed the typical value expected. The AR6A System design compensates for these extreme cases by allowing sufficient margin. The overall intermodulation level in a switch section is monitored. When limits are exceeded, the monitoring system can identify the transmitter or transmitters that require adjustment. In a typical switch section, the random aging and temperature conditions result in an overall switch section performance that satisfies objectives.

V. ACKNOWLEDGMENTS

The authors wish to acknowledge D. R. Rice, H. Miedema, and R. I. Felsberg for their important early contributions.

REFERENCES

1. H. Miedema and R. I. Felsberg, private communication.
2. H. Seidel, "A Microwave Feed-Forward Experiment," B.S.T.J., *50*, No. 9 (November 1971), pp. 2879–916.
3. P. Hetracul and D. P. Taylor, "Compensators for Bandpass Nonlinearities in Satellite Communications," IEEE Trans. Aerosp. Electron. Sys., *12*, No. 4 (July 1976), pp. 509–14.
4. A. R. Kaye, D. A. George, and M. J. Eric, "Analysis and Compensation of Bandpass Nonlinearities for Communications," IEEE Trans. Commun., *20*, No. 5 (October 1972), pp. 965–72.

5. Y. L. Kuo, private communication.
6. R. P. Hecken and R. C. Heidt, "Predistortion Linearization of the AR 6A Transmitter," Int. Conf. Commun., June 8–12, 1980.
7. G. L. Heiter, "Characterization of Nonlinearities in Microwave Devices and Systems," IEEE Trans. Microwave Theory and Techniques, *21*, No. 12 (December 1973), pp. 797–805.
8. R. P. Hecken, U.S. Patent No. 4,157,508, issued June 5, 1979.
9. R. L. Adams, J. L. Donoghue, A. N. Georgiades, J. .R Sundquist, R. E. Sheehey, and C. F. Walker, "The AR6A Single-Sideband Microwave Radio System: System Networks," B.S.T.J., this issue.
10. R. I. Felsberg and M. E. Sands, "The AR6A Single-Sideband Microwave Radio System: Special Test Equipment," B.S.T.J., this issue.

APPENDIX

On the Transfer Function for the Up Converter With a Traveling-Wave Tube

The conversion characteristic of a Schottky diode converter is, for our purposes, most conveniently approximated by the ideal multiplier function

$$z(t) = \mathrm{K} \cdot s(t) \cdot z_{\mathrm{m}}(t), \tag{29}$$

where K is a frequency-independent constant, $s(t)$ the local oscillator (pump) signal, and $z_{\mathrm{m}}(t)$ the modulating (IF) signal. With $s(t) = \cos \omega_o t$, one can see that eq. (29) represents a double-sideband signal with suppressed carrier. Since the bandpass filter following the converter in the actual transmitter suppresses the unwanted sideband, as well as any residual carrier, the use of eq. (29) is indeed justified. Applying a single-tone modulating signal $z_{\mathrm{m}}(t) = A_{\mathrm{m}} \cos(\omega_{\mathrm{m}} t + \phi_{\mathrm{m}})$, one obtains from eq. (29) the lower single-sideband (SSB) signal

$$z(t) = \frac{A_{\mathrm{m}}}{2} \mathrm{K}\ Re\{e^{j(\omega_o - \omega_{\mathrm{m}})t} \cdot e^{-j\phi_{\mathrm{m}}}\}, \tag{30a}$$

and the upper SSB signal

$$z(t) = \frac{A_{\mathrm{m}}}{2} \mathrm{K}\ Re\{e^{j(\omega_o + \omega_{\mathrm{m}})t} \cdot e^{+j\phi_{\mathrm{m}}}\}. \tag{30b}$$

The converter, thus, not only translates the modulating frequency to the desired RF band, but also causes the conjugation of the modulating signal phase. One may, therefore, define two ideal converter transfer operations linking the two frequency domains as follows:

$$Z_{\mathrm{LSB}} = Z(\omega_o - \omega_{\mathrm{m}}) = \mathrm{K_c} \cdot \check{Z}_{\mathrm{m}}(\omega_{\mathrm{m}}) \qquad \text{(LSB)} \tag{31a}$$

and

$$Z_{\mathrm{USB}} = Z(\omega_o + \omega_{\mathrm{m}}) = \mathrm{K_c} \cdot Z_{\mathrm{m}}(\omega_{\mathrm{m}}) \qquad \text{(USB)}, \tag{31b}$$

where $\check{Z}$ is the complex conjugate of Z, and $\mathrm{K_c}$ a frequency-independent constant. Note that these operations describe the combined functions

of up converter and bandpass filter. Introducing eq. (31a) into the nonlinear transfer function, eq. (4) of the main text, yields (with some simplifications)

$$Y_{\mathrm{LSB}} = H_B(B_1 H_A \check{Z}_{\mathrm{m}} + B_3(H_A \check{Z}_{\mathrm{m}})^{3^*}) \tag{32a}$$

and

$$Y_{\mathrm{USB}} = H_B(B_1 H_A Z_{\mathrm{m}} + B_3(H_A Z_{\mathrm{m}})^{3^*}). \tag{32b}$$

With these expressions we have derived nonlinear transfer functions for the cascade of up converter, bandpass filter, and TWT. Note that for the LSB and the USB case, the modulating signal is Z_{m} and it is the converter that performs the conjugation. It also must be mentioned that for the intentions of this model, the converter constant K_c and the transfer function of the bandpass filter have tacitly been absorbed in H_A.

AUTHORS

Rudolf P. Hecken, M.S.E.E., 1959, Ph.D., 1964, Technische Hochshule Aachen, West Germany; Institute for High Frequency Technology, Aachen, 1959–1964; CERN, Geneva, Switzerland, 1964–1968; Bell Laboratories, 1968—. Mr. Hecken has been involved in the design of networks for the L5 coaxial system, FM microwave radio systems, and AR6A Radio System. Since 1982 he has been Director of the Radio Systems and Terminals Laboratory.

Richard C. Heidt, A.S.E.E., Arlington State Jr. College, 1956; B.S.E.E., Southern Methodist University, 1959; M.E.E., New York University, 1963; Bell Laboratories, 1961—. Mr. Heidt was first engaged in microwave transmission circuits and antennas. Since 1969 he has been involved in the design of transmitters for the single-sideband microwave radio system. He is currently Supervisor of a group developing digital microwave radio systems. Member, IEEE, Eta Kappa Nu, Sigma Tau, Kappa Mu Epsilon.

David E. Sanford, E.T., RCA Institutes, 1968; Fairleigh Dickinson University, 1969–1971; Merrimack College, 1982—; Bell Laboratories, 1968—. Mr. Sanford initially worked in the field of plasma physics and was involved in development of transmitter and receiver circuitry for single-sideband radio. Recently he has developed circuits for the receiver portion of digital radio systems.